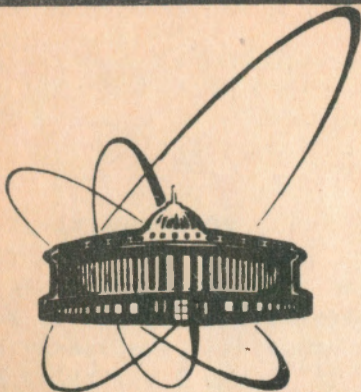


92-68



сообщения
объединенного
института
ядерных
исследований
дубна

E1-92-68

Z.Strugalski, M.Sultanov*

CHARACTERISTICS OF THE PION PRODUCTION
AND PROTON EMISSION PROCESSES
IN PROTON-CARBON NUCLEAR COLLISIONS
AT 4.2 GeV/c MOMENTUM

*SamSU, Uzbekistan

1992

Стругальски З., Султанов М.

E1-92-68

Характеристики процессов рождения

пионов и испускания протонов в протон-углерод
ядерных столкновениях при импульсе 4,2 ГэВ/с

Получены характеристики интенсивности рождения пионов и испускания протонов в протон-ядерных столкновениях при импульсе 4,2 ГэВ/с в зависимости от толщины слоя внутриядерной материи, вовлеченной в реакцию. Наблюдаются пионы с большими поперечными импульсами, больше чем $\sim 1,2$ ГэВ/с.

Работа выполнена в Лаборатории высоких энергий ОИЯИ.

Сообщение Объединенного института ядерных исследований. Дубна 1992

Strugalski Z., Sultanov M.

E1-92-68

Characteristics of the Pion Production
and Proton Emission Processes in Proton-Carbon
Nuclear Collisions at 4.2 GeV/c Momentum

The intensities of the pion production and proton emission in p-carbon collisions at 4.2 GeV/c momentum are obtained in dependence on the intranuclear matter layer thickness involved in the collision reaction. Pions with large transversal momenta, larger than about 1.2 GeV/c, are presented in the reactions.

The investigation has been performed at the Laboratory of High Energies, JINR.

1. INTRODUCTION

The aim of this work has been to gain insight in the physics of the nucleon emission and pion production processes in hadron-nucleus collisions. The experimental data were collected using the 2 meter long propane bubble chamber of the Joint Institute for Nuclear Research exposed to 4.2 GeV/c momentum proton beams. The investigations are performed additionally to our similar works performed by means of xenon bubble chambers irradiated in pion beams at 2.34 - 9 GeV/c momentum.

The intensities of the emitted protons and of the produced pions are studied first of all. As the measure of the proton emission intensity the multiplicity of the emitted protons is used; the intensity of the produced pions is expressed by the multiplicity of the ejected pions in any of the collision events under study.

According to experimental data obtained in our investigations of the hadron-nucleus collisions in the xenon bubble chambers^{/1,2/}, the number of the nucleons emitted from the target nucleus in a collision determines the collision impact parameter; larger number of the emitted nucleons corresponds to smaller value of the collision impact parameter. Approximately, the number of the emitted protons only can be used instead of the numbers of the emitted nucleons. The distributions of the multiplicities of the produced pions at definite numbers of the emitted protons contain information about the pion production process, and the distributions of the multiplicities of the emitted protons in events with various numbers of the ejected pions contain information about the nucleon emission process in the collisions under study.

2. EXPERIMENTAL PROCEDURE

The photographs of the 2 m propane bubble chamber exposed to 4.2 GeV/c momentum proton beams from the Joint Institute for Nuclear Research Synchrophasotron were scanned and rescaned for the p-C collision events which could occur in a chosen region centered inside the chamber. The methodical ques-

tion concerning the expositions of the chamber and the analysis of the photographs are described in former works³⁻⁵; the selection criteria are described as well^{1,7}, they are:

$$n_+ - n_- > 1 + Z_{Ai}, \quad (1)$$

$$n_p > 1, \quad (2)$$

$$n_p^b > 0, \quad (3)$$

$$n_- > 1, \quad (4)$$

$$n_\pm - \text{odd}, \quad (5)$$

where n_+ is the number of positively charged particles in the event; n_- , the number of the negatively charged particles in the event; n_p , the number of the protons with $P_{lab} < 0.75$ GeV/c momentum; n_p^b , the number of protons ejected into backward hemisphere in lab system.

In total, 7328 p-C collision events were selected which makes 82% of the all p-C₃H₈ collisions registered on the chamber photographs under analysis and fulfilled the selection criteria. The lower limit of the momentum value of the emitted protons was $P_{lab} \approx 150$ MeV/c; it is known that protons may be distinguished by ionization from the pions when of momenta $P_{lab} \leq 800$ MeV/c; pions with $P_{lab} \geq 800$ MeV/c can be identified by delta-electrons. The positively one-charged particles with the momentum $P_{lab} \geq 800$ MeV/c were accepted to be protons; the admixture of the positively charged pions in such "proton" sample is about⁵ 12%.

3. EXPERIMENTAL DATA

The collision reactions $p + C_6^{12} \rightarrow n_p + n_{pi} + f$ were studied; n_p is the number of the emitted protons, n_{pi} is the number of the ejected pions with negative and positive charge, f are secondary hadrons if not protons or pions.

In tables I and II general characteristics of the experimental material are presented. In figures 1 - 6 characteristics of the emitted protons are shown in dependence on the multiplicities n_{pi} of the produced pions. In figures 7 - 12 characteristics of the ejected pions are given in dependence on the numbers n_p of the emitted protons. The characteristics of the distributions in figs. 1 - 12 contain tables III - XIV.

Table I. Numbers N_{ev} of collision events and numbers N_{pi} of the produced pions in dependence on the multiplicity n_p of protons emitted in a collision; in parentheses - the numbers without corrections for the efficiency

n_p	0	1	2	3	4	5	6	≥ 0
N_{ev}	310	2814	2342	1011	451	277	94	7328 (5285)
N_{pi}^\pm	338	1120	1342	978	523	332	121	4754

Table II. Numbers N_{ev} of collision events and of the emitted protons N_p in dependence on the multiplicity n_{pi}^\pm of the produced pions; in parentheses - the numbers without correction for registration efficiency

n_{pi}^\pm	0	1	2	3	4	5	≥ 0
N_{ev}	2441	1620	886	316	81	17	7328 (5285)
N_p	3154	3117	1838	688	210	37	9044

Table III. Characteristics of the distributions shown in fig. 1

n_{pi}	N_{ev}	$\langle n_p \rangle$	s.d.	skewness	kurtosis
≥ 0	7328	1.48	1.26	1.2342	1.8299
0	2441	1.39	1.20	1.4768	2.0887
1	1620	1.77	1.50	0.6687	0.3576
2	885	1.90	1.49	0.7775	0.1320
3	316	1.95	1.51	0.6757	0.5975
4	81	2.30	1.46	0.1611	-0.3871
5	17	2.03	1.85	0.7050	-0.0795

Table IV. Characteristics of the distributions shown in fig.2

n Pi	N _p	$\langle P_p \text{ tot} \rangle$	s.d.	skewness	kurtosis
≥ 0	9048	0.720	0.626	1.1771	0.2452
0	3154	0.731	0.636	1.1360	0.1236
1	3117	0.723	0.637	1.1845	0.2249
2	1838	0.730	0.626	1.1540	0.1568
3	688	0.673	0.562	1.2981	0.8543
4	210	0.636	0.505	1.1431	0.3082
5	37	0.586	0.468	1.6105	2.2587

Table V. Characteristics of the distributions shown in fig.3

n Pi	N _p	$\langle P_p \text{ lon} \rangle$	s.d.	skewness	kurtosis
≥ 0	8594	0.436	0.567	1.0838	0.1365
0	2991	0.429	0.579	1.0566	0.0142
1	2944	0.435	0.567	1.1241	0.2331
2	1742	0.454	0.569	1.0795	0.1245
3	667	0.428	0.520	1.0280	0.1614
4	209	0.438	0.524	1.0124	0.0860
5	36	0.349	0.256	1.7744	0.5808

Table VI. Characteristics of the distributions shown in fig.4

n Pi	N _p	$\langle P_p \text{ tr} \rangle$	s.d.	skewness	kurtosis
≥ 0	10854	0.349	0.256	1.7744	4.9630
0	4427	0.352	0.261	1.6978	4.3445
1	3474	0.350	0.253	1.7669	5.0459
2	1991	0.348	0.256	1.9606	6.5374
3	712	0.345	0.245	1.5982	3.0791
4	210	0.336	0.262	2.2118	7.0630
5	37	0.247	0.152	0.8990	0.5400

Table VII. Characteristics of the distributions shown in fig.5

n Pi	N _p	$\langle E_k \rangle$	s.d.	skewness	kurtosis
≥ 0	9737	0.459	0.619	1.6092	1.5869
0	3479	0.509	0.670	1.4656	0.9753
1	3342	0.453	0.611	1.5781	1.4552
2	1956	0.446	0.599	1.6482	1.8320
3	709	0.345	0.474	2.0024	3.6716
4	210	0.269	0.334	1.5736	1.7506
5	37	0.229	0.312	2.3456	5.4741

Table VIII. Characteristics of the distributions presented in fig.6

n Pi	N _p	$\langle \cos \theta_p \rangle$	s.d.	skewness	kurtosis
≥ 0	10862	0.5633	0.5016	-1.2851	0.6486
0	4431	0.5971	0.5036	-1.4116	0.9662
1	3475	0.5372	0.5040	-1.1752	0.3555
2	1991	0.5496	0.4889	-1.2525	0.6716
3	714	0.5254	0.4987	-1.1917	0.3656
4	210	0.5321	0.5018	-1.2755	0.6628
5	37	0.6175	0.4848	-2.0022	3.1499

Table IX. Characteristics of the distributions shown in fig.7

n _p	N _{ev}	$\langle n_{Pi} \rangle$	s.d.	skewness	kurtosis
≥ 0	7328	1.38	0.97	1.0593	0.9737
0	310	2.13	0.83	1.3954	0.8320
1	2814	1.24	0.86	1.2432	0.8600
2	2342	1.28	0.98	1.0201	0.9797
3	1011	1.53	1.03	1.0534	1.0311
4	451	1.65	1.08	0.8103	1.0769
5	277	1.68	1.08	0.9500	1.0831
6	94	1.76	0.93	0.2581	0.9333

Table X. Characteristics of the distributions shown in fig.8

n_p	N_{Pi}	$\langle P_{Pi\ tot} \rangle$	s.d.	skewness	kurtosis
≥ 0	4783	0.43	0.29	1.3412	0.2877
0	339	0.45	0.24	0.8950	0.2448
1	1120	0.46	0.28	1.2310	0.2835
2	1324	0.46	0.30	1.2816	0.2974
3	978	0.43	0.28	1.3854	0.2832
4	523	0.41	0.31	1.6772	0.3085
5	332	0.38	0.28	1.5701	0.2793
6	120	0.36	0.25	1.4710	0.2504

Table XI. Characteristics of the distributions shown in fig.9

n_p	N_{Pi}	$\langle P_{Pi\ lon} \rangle$	s.d.	skewness	kurtosis
≥ 0	4709	0.28	0.28	0.5610	0.2817
0	336	0.32	0.26	0.2036	0.2566
1	1103	0.33	0.27	0.4762	0.2771
2	1299	0.30	0.29	0.4740	0.2863
3	960	0.26	0.28	0.6215	0.2768
4	514	0.23	0.29	0.8348	0.2850
5	330	0.22	0.28	0.8830	0.2788
6	120	0.20	0.27	1.2059	0.2654

Table XII. Characteristics of the distributions shown in fig.10

n_p	N_{Pi}	$\langle P_{Pi\ tr} \rangle$	s.d.	skewness	kurtosis
≥ 0	4810	0.24	0.16	1.3828	0.1574
0	342	0.25	0.15	1.2271	0.1542
1	1124	0.23	0.15	1.3719	0.1451
2	1333	0.24	0.16	1.2307	0.1560
3	983	0.25	0.16	1.4462	0.1617
4	527	0.25	0.17	1.3790	0.1701
5	333	0.23	0.17	1.6427	0.1639
6	120	0.24	0.17	1.6586	0.1676

Table XIII. Characteristics of the distributions shown in fig.11

n_p	N_{Pi}	$\langle E_{k Pi} \rangle$	s.d.	skewness	kurtosis
≥ 0	4794	0.33	0.28	1.6371	0.2792
0	339	0.35	0.25	1.5398	0.2474
1	1122	0.35	0.27	1.4728	0.2722
2	1328	0.35	0.29	1.6674	0.2913
3	979	0.32	0.27	1.6083	0.2732
4	526	0.31	0.30	1.8983	0.3014
5	332	0.28	0.27	1.7348	0.2655
6	120	0.26	0.24	1.6953	0.2380

Table XIV. Characteristics of the distributions shown in fig.12

n_p	N_{Pi}	$\langle \cos \theta_{Pi} \rangle$	s.d.	skewness	kurtosis
≥ 0	4811	0.5491	0.4827	-1.4253	0.4827
0	342	0.6259	0.4194	-1.7760	0.4194
1	1125	0.6293	0.4318	-1.7472	0.4318
2	1333	0.5764	0.4625	-1.4957	0.4625
3	983	0.5142	0.4974	-1.2835	0.4974
4	527	0.4403	0.5308	-1.0884	0.5308
5	333	0.4438	0.5342	-1.0659	0.5342
6	120	0.3880	0.5322	-1.1327	0.5322

4. DISCUSSION AND RESULTS

Experimental results are presented in figs.1-12. The most interesting fact is: pions with large transversal momenta, larger than about 1.2 GeV/c, are presented in the transversal momentum spectra (Fig.10).

The admixture of the beam protons among the protons accepted as the emitted ones is visible clearly, figs.2,3,4,5,6; it amounts about 15-20%. It should be taken into account in investigating the proton or nucleon emission process on the basis of nucleon-nucleus collision experimental data at momenta of about a few GeV.

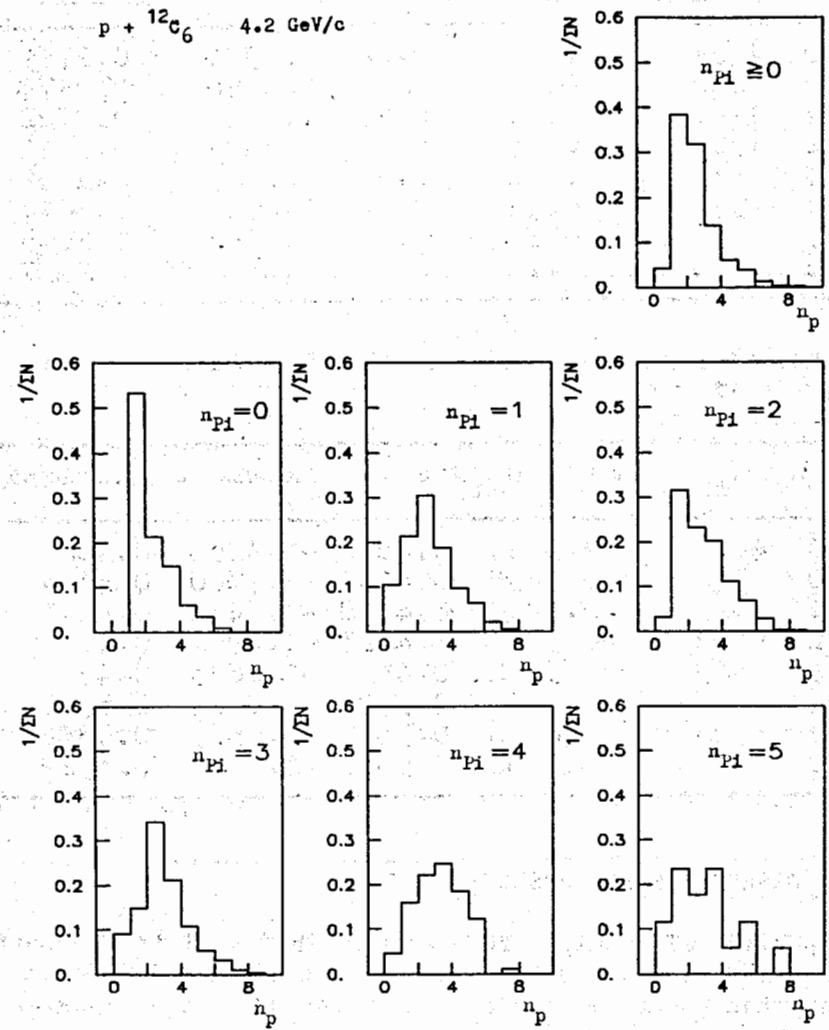


Fig.1. Emitted protons multiplicity n_p distributions
 $N(n_p) = 1/\Sigma N$, in samples of collision events with various multiplicities n_{pi} of ejected charged pions

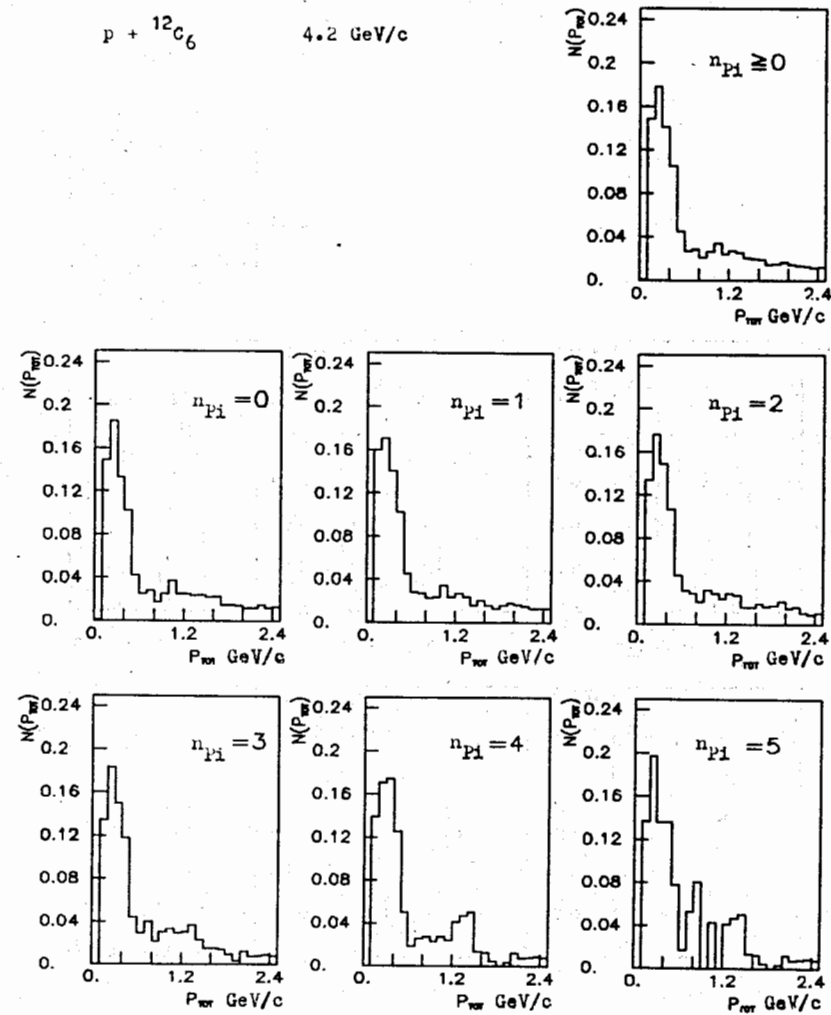


Fig.2. Emitted protons total momenta P_{tot} distributions $N(P_{tot})$, in events with various multiplicities n_{pi} of ejected charged pions

$p + {}^{12}C_6$ 4.2

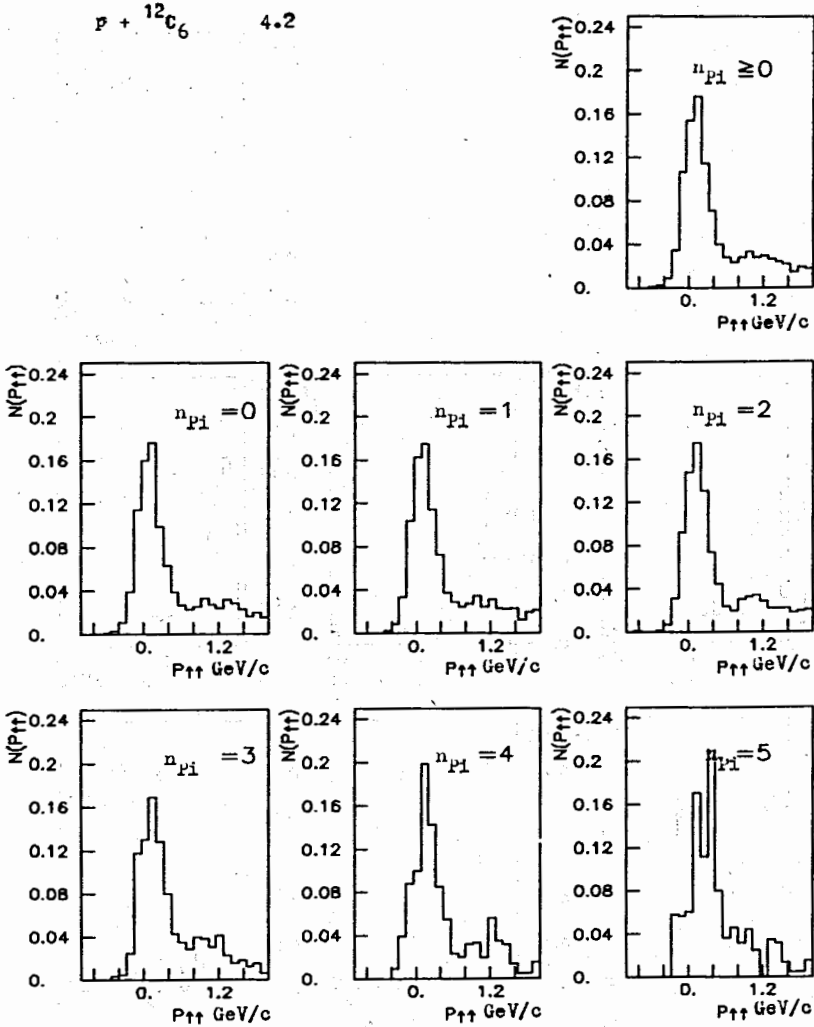


Fig.3. Emitted protons longitudinal momenta $P_{1\text{on}} = P_{11}$ distributions $N(P_{11})$ in events with various multiplicities n_{pi} of the ejected charged pions

$p + {}^{12}C_6$ 4.2 GeV/c

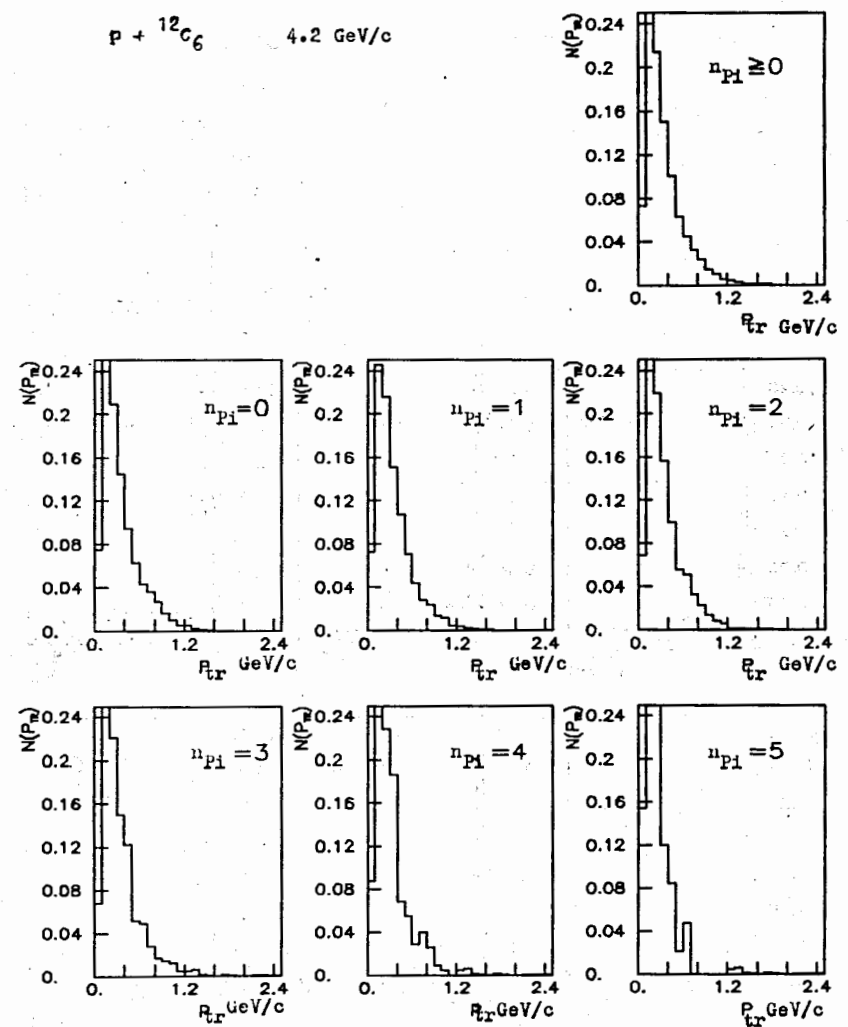


Fig.4. Emitted protons transversal momenta P_{tr} distributions $N(P_{tr})$ in events with various multiplicities n_{pi} of the ejected pions

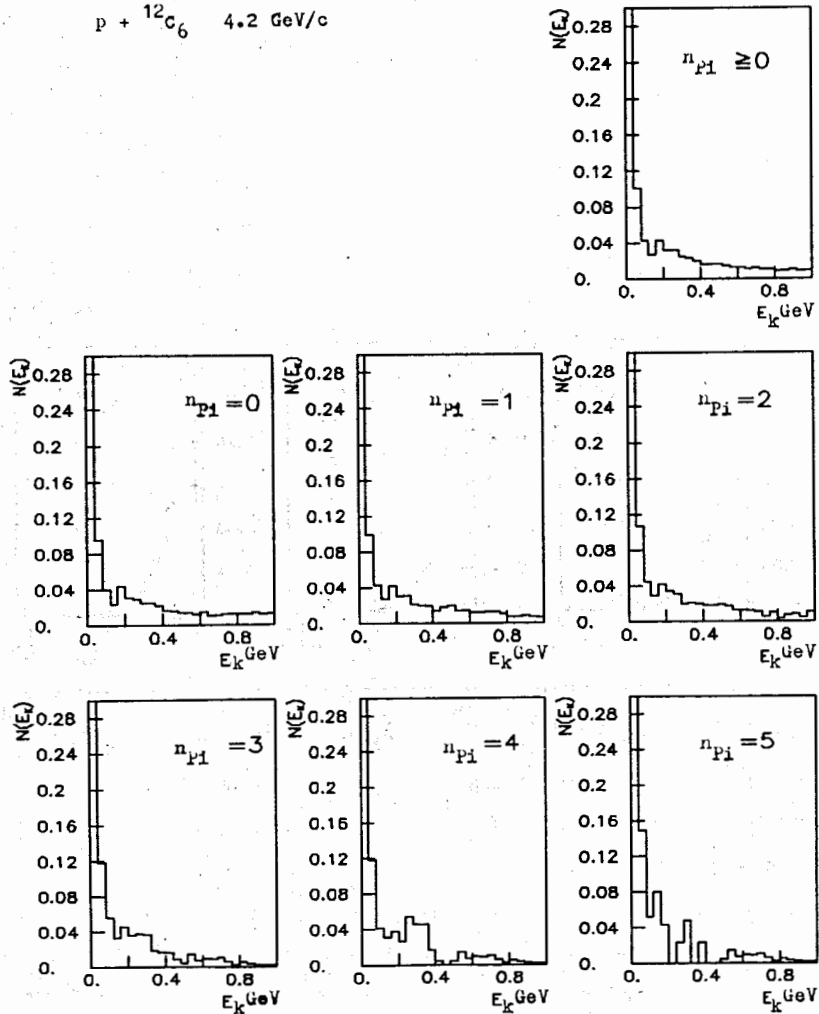


Fig.5. Emitted protons kinetic energy E_k distributions $N(E_k)$ in events with various multiplicities n_{pi} of the ejected pions

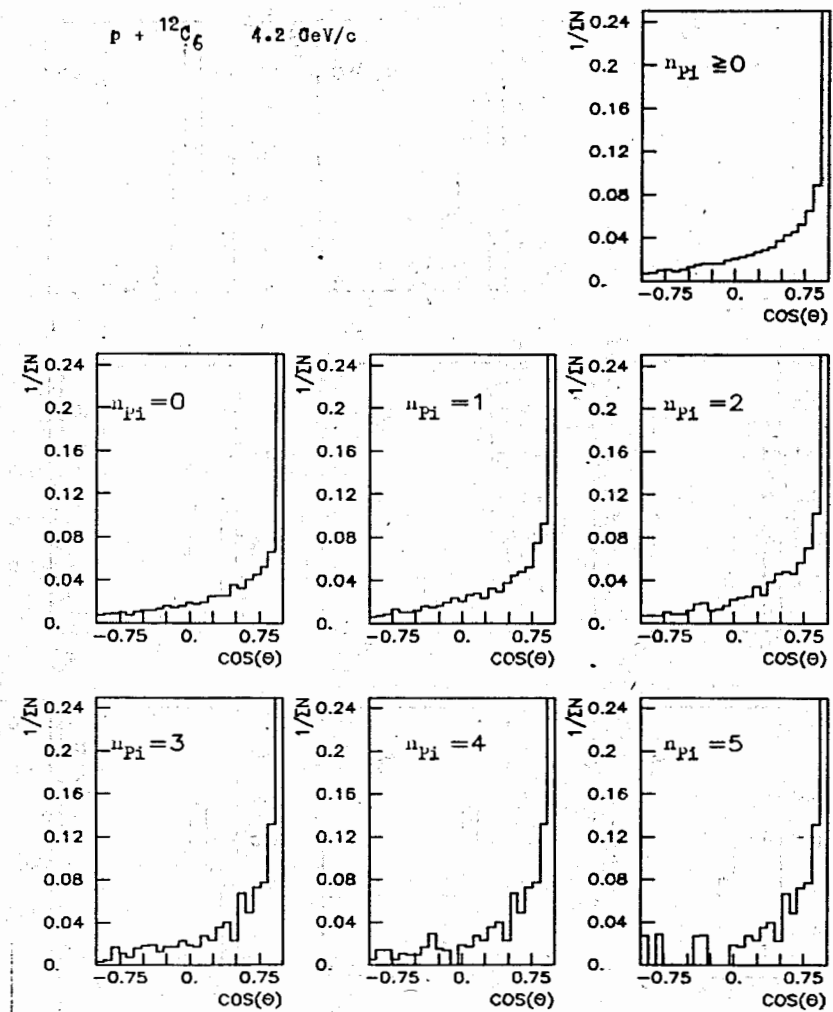


Fig.6. Emitted protons emission angle θ distributions $N(\cos \theta) = 1/\Sigma$ in events with various multiplicities n_{pi} of the ejected pions

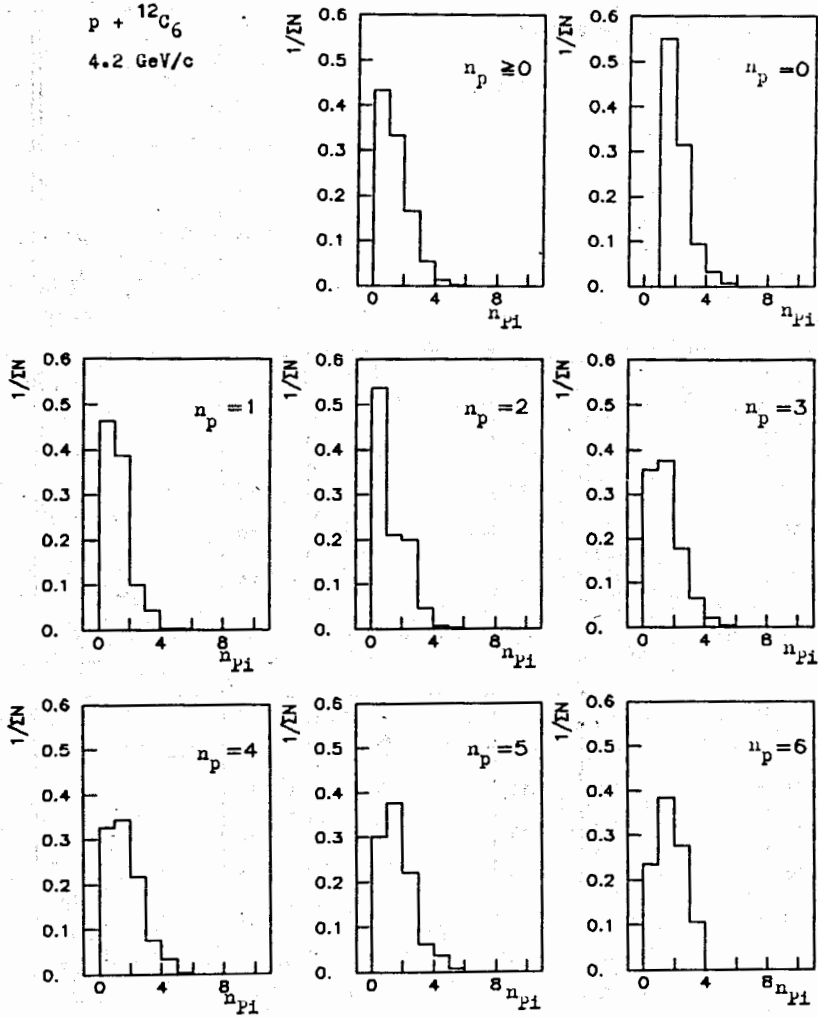


Fig.7. Ejected pions multiplicity n_{π} distributions $N(n_{\pi}) = 1/\Sigma N$ in events with multiplicities n_p of the emitted protons

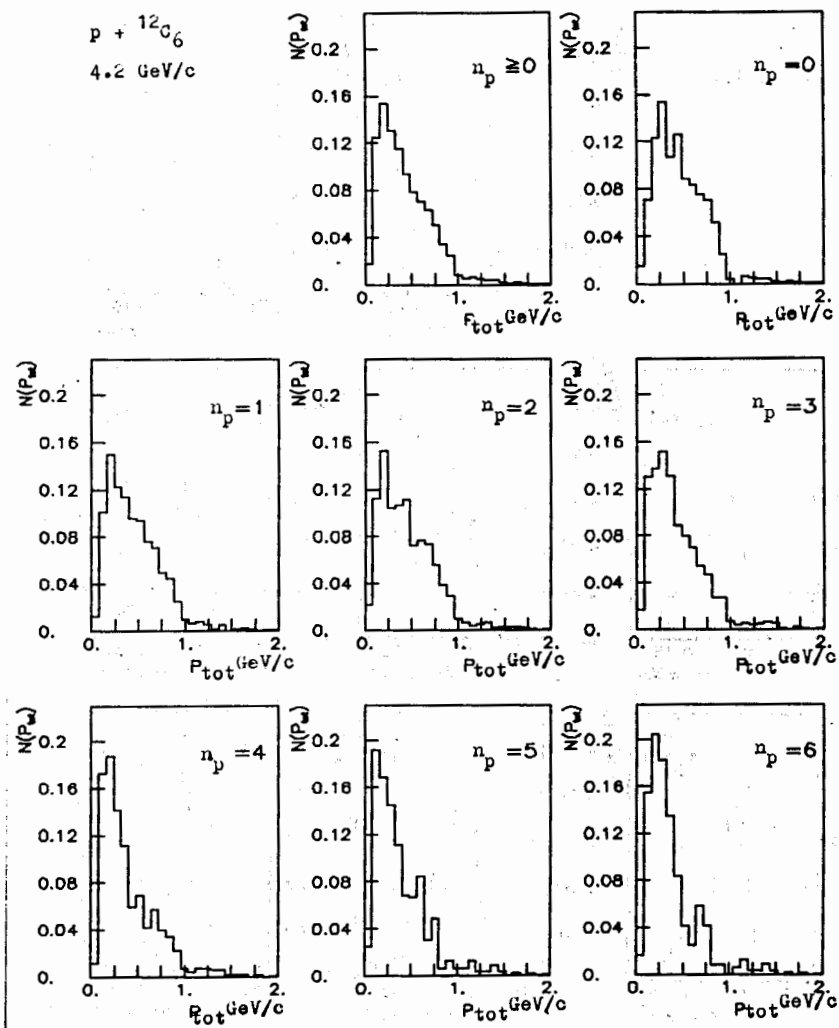


Fig.8. Ejected pions total momenta P_{tot} distributions $N(P_{\text{tot}})$ in events with various multiplicities n_p of the emitted protons

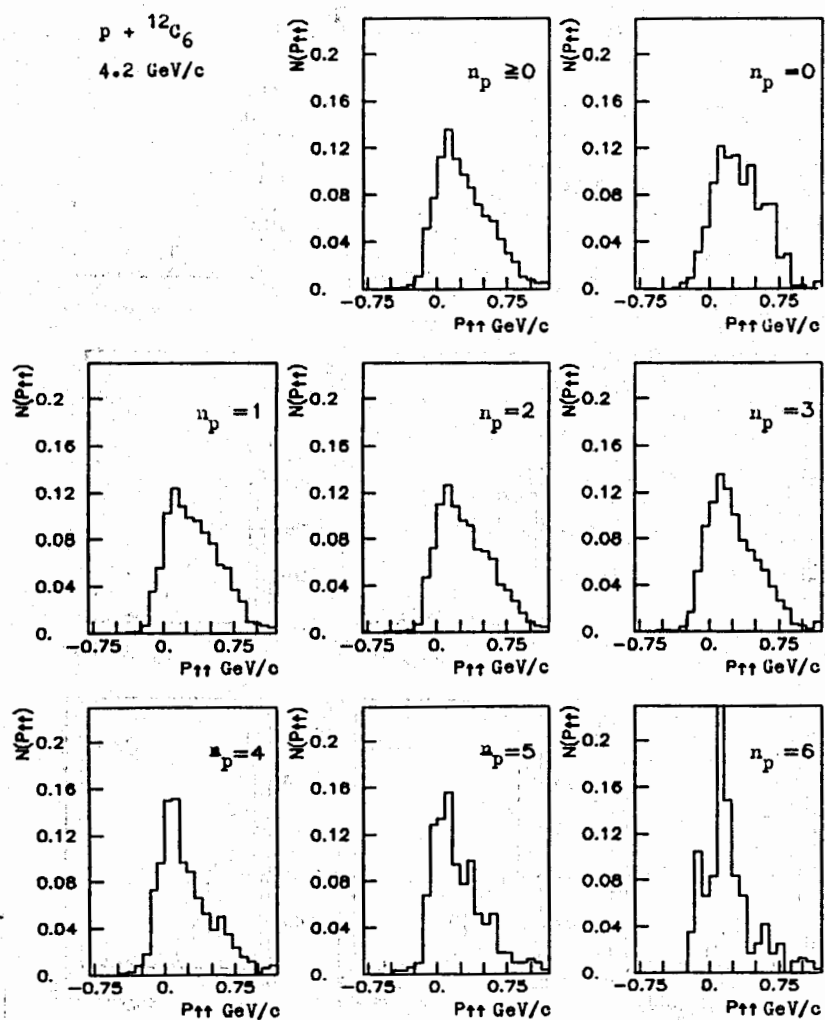


Fig.9. Ejected pions longitudinal momenta P_{11} distributions $N(P_{11})$, in events with various multiplicities n_p of the emitted protons

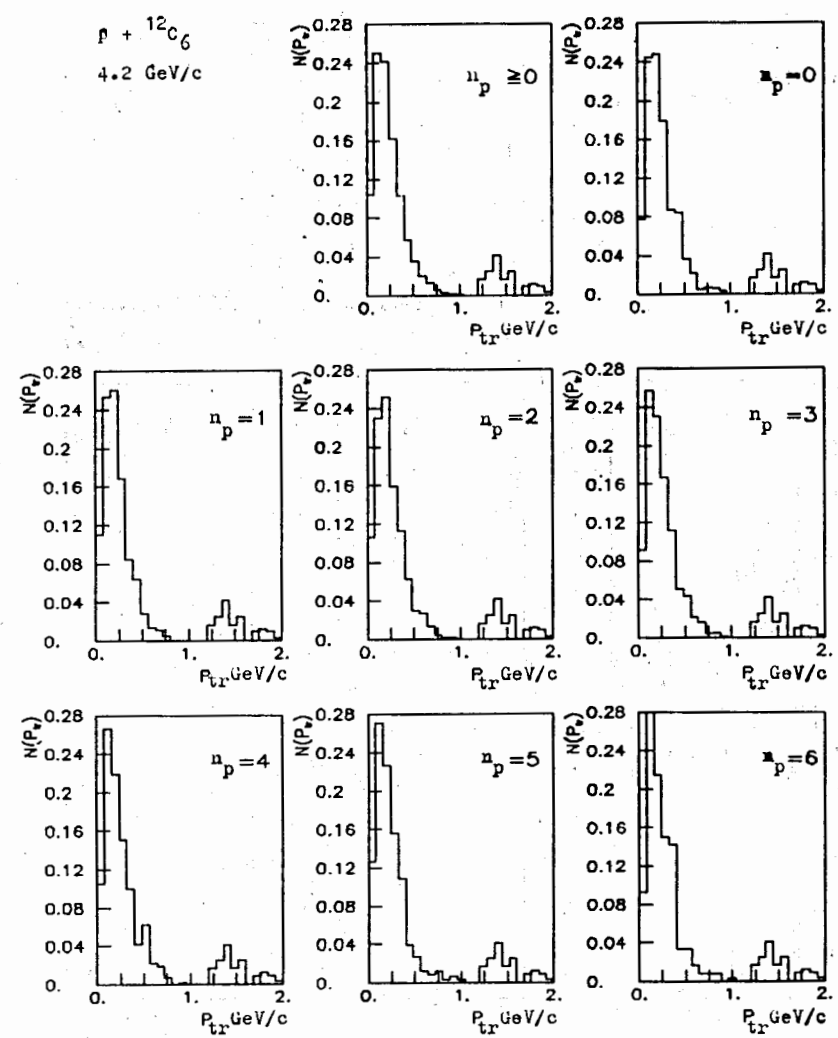


Fig.10. Ejected pions transversal momenta P_{tr} distributions $N(P_{tr})$ in events with various multiplicities n_p of the emitted protons

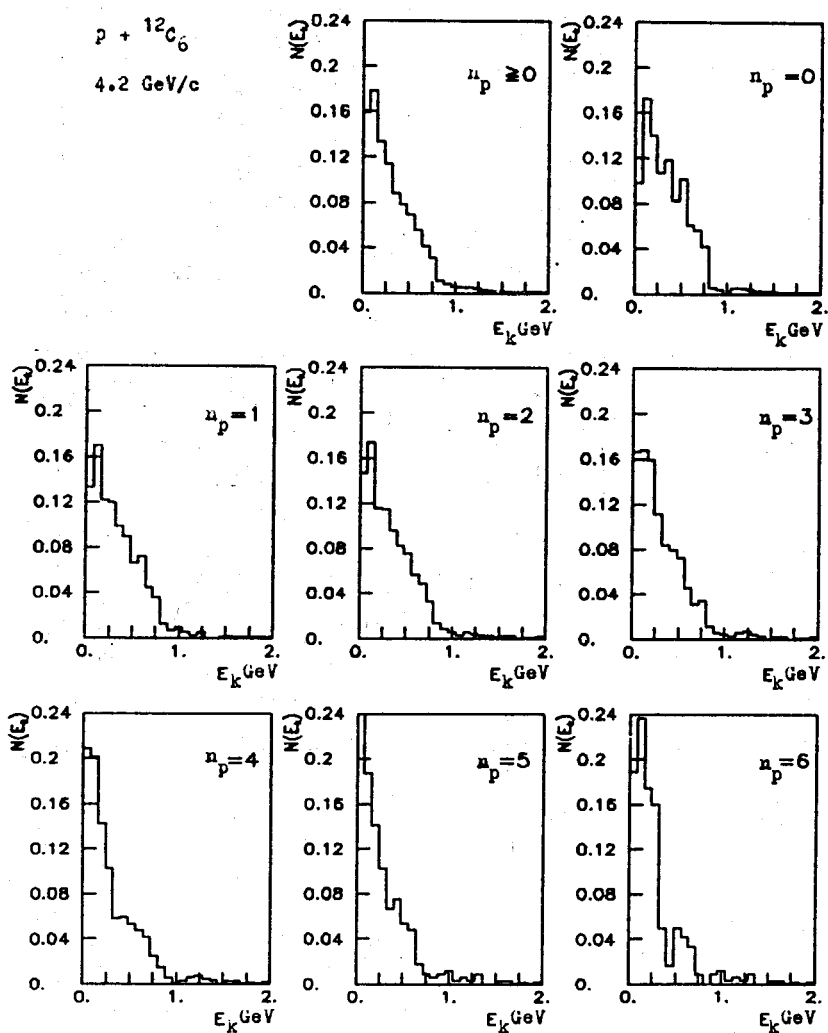


Fig.11. Ejected pions kinetic energy E_k distributions $N(E_k)$ in events with various multiplicities n_p of the emitted protons

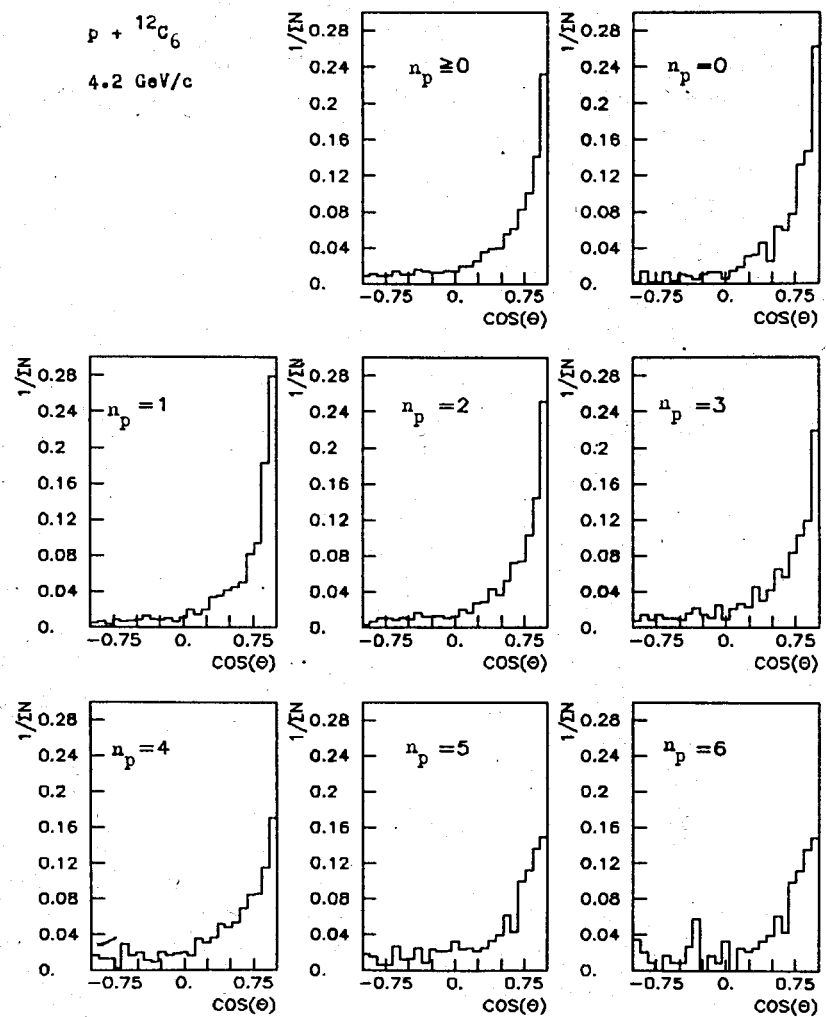


Fig.12. Ejected pions emission angle θ distributions $N(\cos \theta) = 1/\Sigma N$ in events with various multiplicities n_p of the emitted protons

REFERENCES

1. Strugalski Z. - JINR E1-81-576, E1-81-577, Dubna, 1981.
2. Strugalski Z. et al. - JINR E1-90-459, Dubna, 1990.
3. Abdurakhimov E.O. et al. - JINR P1-10779, Dubna, 1977.
4. Gasparian A.P. et al. - JINR P1-80-778, Dubna, 1980.
5. Baldin A.M. et al. - JINR P1-88-331, Dubna, 1988.
6. Agakishiev G.I. et al. - JINR P1-83-662, Dubna, 1983.
7. Kladnitskaya E.N. et al. - JINR P1-88-412, Dubna, 1988.

Received by Publishing Department
on February 21, 1992.